Emergent interacting phases in the strong-coupling limit of twisted M-valley moiré systems: Application to $SnSe_2$

Ming-Rui Li,[1,2] Dumitru Calugaru,[3] Yi Jiang,[4] Hanqi Pi,[4] Ammon Fischer,[5] Henning Schlömer,[6,7] Lennart Klebl,[8] Zhengchao Xia,[9] Maia G. Vergniory,[10,4] Dante M. Kennes,[5,11,12] Kin Fai Mak,[9,5] Jie Shan,[9,5] Siddharth A. Parameswaran,[3] Hong Yao,[1] B. Andrei Bernevig,[2,4,13,*] and Haoyu Hu[2,†]

[1] *Institute for Advanced Study, Tsinghua University, Beijing 100084, China*
[2] *Department of Physics, Princeton University, Princeton, NJ 08544, USA*
[3] *Rudolf Peierls Centre for Theoretical Physics, University of Oxford, Oxford OX1 3PU, United Kingdom*
[4] *Donostia International Physics Center (DIPC), Paseo Manuel de Lardizábal. 20018, San Sebastián, Spain*
[5] *Max Planck Institute for the Structure and Dynamics of Matter, Luruper Chaussee 149, 22761 Hamburg, Germany*
[6] *Department of Physics and Arnold Sommerfeld Center for Theoretical Physics (ASC), Ludwig-Maximilians-Universität München, Theresienstr. 37, München D-80333, Germany*
[7] *Munich Center for Quantum Science and Technology (MCQST), Schellingstr. 4, München D-80799, Germany*
[8] *Institute for Theoretical Physics and Astrophysics and Würzburg-Dresden Cluster of Excellence ct.qmat, University of Würzburg, 97074 Würzburg, Germany*
[9] *School of Applied and Engineering Physics and Laboratory of Atomic and Solid State Physics, Cornell University, Ithaca, NY, USA*
[10] *Département de Physique et Institut Quantique, Université de Sherbrooke, Sherbrooke, J1K 2R1 Québec, Canada*
[11] *Center for Computational Quantum Physics (CCQ), The Flatiron Institute, New York, New York 10010, USA*
[12] *Institut f¨ur Theorie der Statistischen Physik, RWTH Aachen, 52056 Aachen, Germany and JARA - Fundamentals of Future Information Technology*
[13] *IKERBASQUE, Basque Foundation for Science, 48013 Bilbao, Spain*

We establish twisted $SnSe_2$ as a tunable platform for simulating dimension-dependent correlated physics, distinct from conventional K-valley moiré systems. By constructing interacting Wannier models, we show that the stacking configuration dictates the effective lattice geometry. In AA-stacked bilayers, a momentum-space nonsymmorphic symmetry constrains the single-particle hopping within each valley to be effectively one-dimensional, while still allowing fully two-dimensional interactions, thereby giving rise to an effective quasi-one-dimensional system. This dimensional reduction stabilizes exotic phases including dimerized states with finite residual entropy, valence bond solids, and quantum paramagnetism. Conversely, AB-stacking maps to a frustrated Kagome lattice; here, strong interactions drive the emergence of a classical spin liquid. The high tunability of this moiré system, which allows control over both the filling and interaction strength (via twist angle), renders twisted $SnSe_2$ a versatile platform for realizing a wide range of exotic correlated quantum phases.

Introduction. The discovery of moiré superlattices has revolutionized the study of strongly correlated systems by providing an unprecedented level of control for engineering electronic phases through the variation of twist angles and stacking configurations [1–5]. The moiré modulation quenches the kinetic energy and drives the system into the strong interaction regime. The high tunability further enables the realization of various exotic many-body phases. In particular, twisted bilayer graphene [6] has been shown to host unconventional superconductivity [7–16], correlated insulators [8–11, 17–43], and other exotic phases [44–60]. It has also emerged as a simulator for topological heavy-fermion physics [61–74]. More recently, multilayer rhombohedral graphene with hBN alignment was also shown to exhibit highly nontrivial correlated and topological physics [75–93]. Beyond graphene-based systems, transition metal dichalcogenide bilayers offer another avenue to realize a wide variety of exotic phases, including correlated insulators [94–97], unconventional superconductors [98–110], integer and fractional Chern insulators [90, 111–135], and other intriguing emerging phases [136–139]. These discoveries highlight the growing potential of moiré materials as a versatile platform for exploring correlated and topological quantum physics.

However, to date, most moiré superlattices have been constructed by twisting monolayers with low-energy electronic states located near the K [6, 94, 140–142] or Γ [143, 144] points of the Brillouin zone (BZ). Recently, a new class of moiré systems based on monolayers with low-energy states at the M points of the BZ has garnered significant interest [145–153]. These M-valley systems feature three time-reversal-preserving valleys related by three-fold rotational symmetry which led to distinct effective lattice models and symmetries compared

* bernevig@princeton.edu
† hh5463@princeton.edu

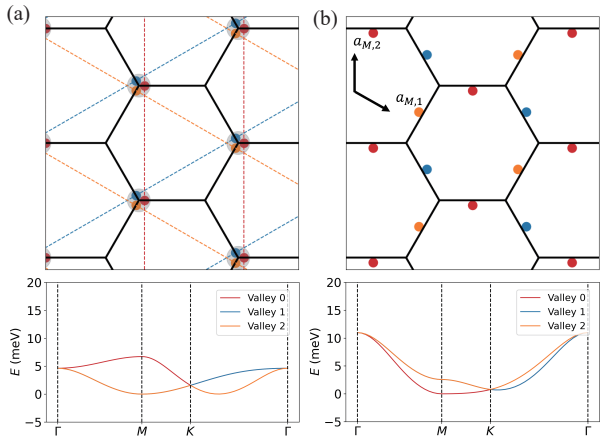

Figure 1. Wannier centers (upper panel) and lowest-band dispersions at $\theta = 3.89°$ (lower panel) of the three valleys for AA-stacked (a) and AB-stacked (b) $SnSe_2$. In the upper panel, solid black lines denote the moiré unit cell boundary. The Wannier centers of valleys 0, 1, and 2 are marked by red, blue, and orange dots, respectively. In panel (a), the dominant intra-valley hoppings are indicated by dashed lines. In panel (b), the three sublattices form an approximate kagome lattice.

to the conventional TMD K-valley moirés. Specifically, twisted bilayers of 1T-$SnSe_2$, among other materials, have been proposed as an experimentally realizable candidate [145, 154]

In this work, we construct interacting Wannier models based on *ab initio* calculations of both AA-stacked and AB-stacked twisted $SnSe_2$ and explore the corresponding correlated physics. In the AA-stacked case, emergent momentum-space non-symmorphic symmetries [145, 155–159] enforce quasi-one-dimensional intra-valley hopping, while inter-valley interactions establish two-dimensional electronic correlations. The constrained kinetic structure is distinct from the more isotropic 2D hopping typical in K-valley moirés. By combining various theoretical methods, we identify several exotic phases, including a dimerized phase with finite residual entropy, valence bond solids, and quantum paramagnetism. For the AB-stacked $SnSe_2$, the Wannier centers of the three valleys form a kagome lattice, providing a direct realization where the valley index maps to the sublattice index. The specific lattice geometry enables us to map the system in the strong coupling limit to a kagome Ising model, where charge occupancy plays the role of the Ising variable. The frustration inherent in the kagome lattice gives rise to strong fluctuations of Ising variables, and stabilizes a classical spin liquid phase.

Interacting Wannier models. To bridge the gap between the continuum moiré bands and strongly correlated lattice physics, we first construct an effective tight-binding description. For both AA-stacked and AB-stacked twisted $SnSe_2$, the lowest conduction bands are topologically trivial in each valley [145], allowing for the construction of exponentially localized Wannier orbitals [160, 161] (Appendix II [162]). The corresponding interactions between Wannier orbitals are obtained by projecting the screened Coulomb repulsion [163] to the Wannier basis (Appendix III [162]).

As shown in Fig. 1, the lattice of Wannier centers (colored dots) exhibit different geometries with the two stacking configurations. In the AA-stacked case (panel (a)), the Wannier centers of the three valleys are nearly coincident, enabling an effective description in terms of a three-orbital triangular lattice Hubbard model (Appendix III 3 [162]). In contrast, for AB-stacked $SnSe_2$, the Wannier centers form an approximate kagome lattice, giving rise to an effective kagome lattice model where the three valleys correspond to three sublattices. Crucially, these models exhibit novel features that distinguish them from conventional triangular and kagome lattice models, as discussed in the following.

For the AA-stacked $SnSe_2$, the kinetic term of the system reveals a striking feature: dimensional reduction driven by symmetry. The Hamiltonian is given by (Appendix III 3 [162]):

$$H_t = \sum_{\mathbf{R},\Delta\mathbf{R},\eta,s} t^{\eta}_{\Delta\mathbf{R}} \hat{d}^{\dagger}_{\mathbf{R},\eta,s} \hat{d}_{\mathbf{R}+\Delta\mathbf{R},\eta,s}, \tag{1}$$

where $\hat{d}^{(\dagger)}_{\mathbf{R},\eta,s}$ annihilates (creates) an electron at moiré unit cell labeled by $\mathbf{R}$ of valley η and spin s. Due to the approximate non-symmorphic symmetry [145], transverse hopping is prohibited. The system exhibits a quasi-1D character, with the dominant hopping amplitude $t^{\eta}_{\Delta\mathbf{R}} = t\delta_{\Delta\mathbf{R},\pm C^{\eta}_{3z}\boldsymbol{a}_{M,2}}$ restricted to specific directions for each valley. This confinement is depicted in Fig. 1 (a), where the dominant hopping directions for the three valleys is indicated with the dashed lines in corresponding, effectively decoupling the 2D layer into independent 1D chains. The interactions, however, restore the 2D correlations. The dominant term is the local repulsion:

$$H_U = \sum_{\mathbf{R},\eta,\eta'} \frac{U_{\eta\eta'}}{2} n_{\mathbf{R},\eta} n_{\mathbf{R},\eta'}, \tag{2}$$

where the density operator is defined as $n_{\mathbf{R},\eta} = \sum_s \hat{d}^{\dagger}_{\mathbf{R},\eta,s} \hat{d}_{\mathbf{R},\eta,s}$. Since the Wannier centers of the three valleys within the same unit cell are nearly coincident, the interaction is approximately $U(6)$-symmetric (with $U_{\eta\eta'} \approx U$), acting purely locally within the moiré unit cell (gray circles in Fig. 1(a)). The subleading interactions are long-range density-density couplings, which remains below 10% of U (Appendix III 3 [162]).

For the Wannier model of AB-stacked $SnSe_2$, the kinetic term retains the form of Eq. (1) with only intra-valley hopping. Unlike the conventional kagome model, nearest-neighbor inter-valley (inter-sublattice) hopping is forbidden. The dominant interactions can be written as

$$H_V = \frac{1}{2} \sum_{\mathbf{R},\Delta\mathbf{R},\eta\eta'} V_{\eta\eta'}(\Delta\mathbf{R}) n_{\mathbf{R},\eta}(\mathbf{R}) n_{\mathbf{R}+\Delta\mathbf{R},\eta'}, \tag{3}$$

which consist of an on-site intra-valley Hubbard interaction $V_{\eta,\eta}(\mathbf{0}) = U$ and a nearest-neighbor inter-valley density-density interaction of strength V_1, where the nearest neighbor is defined with respect to the kagome lattice geometry. Thus, while electrons cannot hop between nearest neighbors, they strongly repel each other across these bonds.

Next, we investigate the correlation physics and quantum phases captured by our interacting Wannier models. Precisely determining the effective dielectric constant in van der Waals heterostructures is inherently difficult due to its sensitivity to the specific experimental environment, including hBN encapsulation [164, 165] and high-energy-band screening [166]. While our first-principles density functional perturbation theory calculations using VASP [167–171] and local-field effects [172, 173] yield an intrinsic static value of $\epsilon_0 \sim 15-30$ (Appendix III [162]), we adopt a baseline of $\epsilon = 12$ and treat the overall interaction scale as a tunable parameter to map the phase diagram.

Hartree-Fock phase diagram of AA-stacked $SnSe_2$. We explore the interacting phase diagram of AA-stacked $SnSe_2$ using momentum-space Hartree-Fock theory. Due to the approximate particle-hole symmetry (Appendix III 3C [162]), we focus on integer fillings $\nu = 1, 2, 3$, where ν represents the number of electrons per moiré unit cell out of six states. The phase diagrams for different interaction strengths (characterized by different dielectric constants ϵ) are presented in Fig. 2 (a,b,c), and can be categorized into three distinct regions: the weak coupling region (gray), the strong coupling region (red), and the flat-band region (blue).

In the weak-coupling region, our Hartree-Fock simulations reveal only gapless phases (Appendix IV [162, 174]). However, we note that the quasi-one-dimensional nature of the hopping derived in the previous section suggests that these gapless states may physically manifest as Luttinger liquids rather than simple Fermi liquids [175–179]. As the interaction strength increases, the system enters the strong-coupling regime, where charge degrees of freedom become gapped due to the strong interaction. Crucially, while charge is localized, the spins remain coupled via a super-exchange interaction of order t^2/U, which stabilize a robust antiferromagnetic (AFM) order effectively described by a Heisenberg model. This regime is physically relevant to the dielectric constant we obtained via DFPT, placing realistic samples within this strong coupling window. Finally, in the ultra-strong coupling limit (blue regions), the Heisenberg exchange coupling t^2/U is strongly suppressed due to the large interaction, distinguishing it from the previous strong-coupling regime. The finite quantum geometry of the bands leads to a ferromagnetic, valley-polarized state [163, 180]. We also note that the ultra-strong coupling regime for $\nu = 3$ emerges at $12/\epsilon > 1.6$ in the small-angle regime (as detailed in Appendix IV [162]).

Quantum spin model in the strong coupling limit of AA-stacked $SnSe_2$. We now focus on the strong-coupling limit. In this regime, Hartree–Fock simulations may underestimate quantum fluctuations, which are further enhanced by the quasi-1D nature of the system. To solve this, we derive the effective quantum spin model that describes this limit and show that it can be solved exactly under proper approximation, revealing a variety of exotic quantum phases.

With the second-order perturbation theory, the effective quantum spin model Hamiltonian (Appendix V [162]) at integer filling $\nu = 1, 2, 3$ reads:

$$H_\nu = \sum_{\mathbf{R},\Delta\mathbf{R},\eta,\eta'} P_L^\nu \frac{\delta V_{\eta\eta'}(\Delta\mathbf{R})}{2} n_{\mathbf{R},\eta} n_{\mathbf{R}+\Delta\mathbf{R},\eta'} P_L^\nu + J \sum_{\mathbf{R},\Delta\mathbf{R},\eta} P_L^\nu \left[\boldsymbol{S}_{\mathbf{R},\eta} \cdot \boldsymbol{S}_{\mathbf{R}+\Delta\mathbf{R},\eta} + \frac{n_{\mathbf{R},\eta} n_{\mathbf{R}+\Delta\mathbf{R},\eta}}{4} \right] P_L^\nu, \tag{4}$$

Here, P_L^ν projects the system onto the low-energy subspace with filling ν. The model includes two types of interactions: a density-density term from the projected Coulomb repulsion $\delta V_{\eta,\eta'}(\Delta\mathbf{R})$ that favors valley polarization, and an intra-valley Heisenberg interaction with coupling $J = 2t^2/(U - V)$, where V is the nearest-neighbor interaction strength. Crucially, due to the quasi-1D property of electron hopping, the corresponding spin coupling is also 1D-like, thus we only keep the dominant nearest-neighbor 1D coupling with $\Delta\mathbf{R} = \pm C_{3z}^\eta \boldsymbol{a}_{M,2}$ for each valley η. The Heisenberg coupling term generally favors antiferromagnetic correlations within each valley. A defining feature of this spin model is that the valley-resolved density $n_{\mathbf{R},\eta}$ remains a local good quantum number. This property allows us to exactly solve the model in two limiting cases (see Appendix V [162]). We first analyze the limit where the classical repulsion is negligible (small $12/\epsilon$, thus $\delta V \approx 0$) For a given density distribution $\{n_{\mathbf{R},\eta}\}$, the system can be effectively described as a collection of open-boundary spin chains. As visualized in Fig. 3(a) with $\nu = 1$ as an example, because the exchange interaction is strictly intra-valley and 1D-like, the 2D triangular lattice physically can be viewed as a set of decoupled chains of varying lengths. Each spin chain is described by a sequence of sites occupied by electrons from the same valley and aligned along a specific direction. Leveraging exact results from the Bethe Ansatz [181–184] and Density Matrix Renormalization Group (DMRG) [185], we can determine the ground state that minimizes the energy for any given configuration $\{n_{\mathbf{R},\eta}\}$. For open-boundary spin chains Eq. (4), the energy per electron is minimized for spin chains of length two. Consequently, the ground state exhibits a strong energetic preference to fragment into length-2 spin-singlet dimers (Appendix V [162]).

For the ground state of $\nu = 1$ (one electron per unit cell), all electrons must pair with a nearest neighbors to form a singlet dimer [186]. In addition, to satisfy the ground state condition, two dimers of the same valley cannot be nearest neighbors along the chain direction

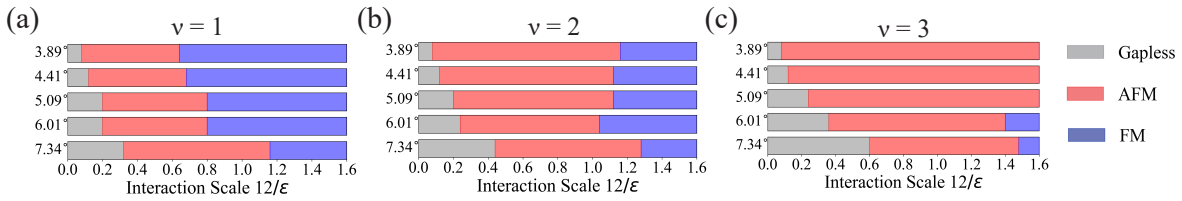

Figure 2. (a) (b) (c) Hartree-Fock phase diagram for $\nu = 1, 2, 3$. In the phase diagram, the gray, red, and blue regions correspond to the weak-coupling (gapless symmetric), strong-coupling (gapped AFM), and flat-band regimes (gapped FM), respectively.

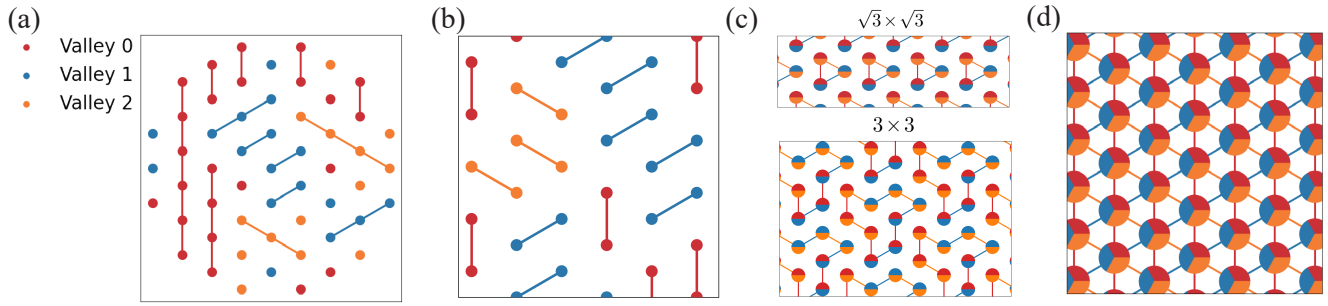

Figure 3. (a) A random $\{n_{\mathbf{R},\eta}\}$ configuration for $\nu = 1$. Each dot represents a unit cell of the system where red, orange and blue denote the unit cell has one electron in valley $0, 1, 2$ respectively. The dots connected by different colors denote the formation of spin chains with various lengths in different valleys. (b) (c) (d) characterize the ground state configurations at filling $\nu = 1, 2, 3$ in the strong coupling limit, respectively. The dots marked with one, two, or three colors represent unit cells occupied by one, two, or three electrons from different valleys, respectively.

$\pm C_{3z}^{\eta} \boldsymbol{a}_{M,2}$ (illustrated in Fig. 3 (b)), as this would effectively form a higher-energy length-4 chain (Appendix V [162]). We find that this constraint leads to a highly degenerate ground state manifold. Consequently, the ground state is not a simple ordered crystal but a disordered state carrying finite zero-temperature entropy. By combining exact diagonalization for small clusters with an analytical mapping to an interacting Majorana fermion model, building on classical dimer/Pfaffian methods [187–189] (Appendix V [162]), we estimate this residual entropy to be $S \approx 0.307 k_B$.

In stark contrast, at $\nu = 2$, the increased density allows the "packing puzzle" to be solved by ordered patterns. We identify that there are only two symmetry-inequivalent ground-state configurations (Appendix V [162]), in which all electrons form spin-singlet dimers. These two configurations correspond to valence-bond–solid (VBS) states exhibiting $\sqrt{3}\times\sqrt{3}$ and 3×3 periodicities, respectively, as visualized in Fig. 3(c). However, at $\nu = 3$, the dimer picture breaks down entirely. With three electrons per site, it is geometrically impossible to partition the system purely into length-2 dimers. As we show in Appendix V [162], the ground state favors the formation of infinitely long spin chains, with each site occupied by one electron from each valley, as illustrated in Fig. 3(d). This state effectively behaves as a bundle of 1D Heisenberg chains, each exhibiting a quantum disordered ground state driven by strong quantum fluctuations.

Finally, we address the robustness of these 1D-derived phases in the realistic 2D material. The strict 1D confinement is an idealization; in reality, subdominant inter-chain hoppings introduce weak 2D couplings. Crucially, our perturbative analysis confirms that these "symmetry-breaking" terms remain orders of magnitude smaller than the dominant intra-chain exchange J (Appendix V 2f and 3e [162]). For the dimerized ($\nu = 1$) and VBS ($\nu = 2$) phases, our perturbative analysis reveals that this coupling generates an effective repulsion between dimers of the same valley on neighboring chains, insufficient to melt the local order. As for $\nu = 3$, the system maps to a spatially anisotropic triangular Heisenberg model; previous numerical studies confirm that the quantum disordered nature of the ground state remains stable against weak inter-chain couplings [152, 190–192]. Thus, the exotic correlations predicted by our 1D model are expected to survive at experimentally relevant temperatures.

In the opposite limit, where $\delta V_{\eta\eta'}(\Delta\mathbf{R})$ dominates over J. the prevalence of $\delta V_{\eta\eta'}$ tends to stabilize valley polarization state (see Appendix V 1b [162])) such that each moiré unit cell is occupied by electrons of the same valley flavor. Dimer formation is thus forbidden, and the system is described by a set of one-dimensional spin chains after including the finite J, each favoring a quantum disordered ground state.

Flat-band limit of AB-stacked $SnSe_2$ and the classical

"spin" liquid. We now explore interaction effects in AB-stacked $SnSe_2$, where the kinetic term is suppressed by the strong coupling limit, and we set the kinetic term to zero. In this regime, the system is effectively described by a classical charge model, with the corresponding Hamiltonian given in Eq. (3), along with an additional chemical potential term $-\mu \sum_{\mathbf{R},\eta} n_\eta(\mathbf{R})$ that controls the filling. To reveal the physics of this kagome model, we map the electronic density $n_\eta(\mathbf{R})$ onto a classical Ising pseudospin variable σ, where empty (0) and filled (1) states correspond to spin-down (-1) and spin-up ($+1$), respectively. Double-occupied states are neglected due to strong on-site Hubbard repulsion. Then, $V_{\eta\eta'}(\Delta\mathbf{R})$ represents the effective Ising coupling, while the chemical potential acts as an effective magnetic field (Appendix VI 1 [162]). Crucially, the interaction matrix $V_{\eta\eta'}(\Delta\mathbf{R})$ encodes the underlying kagome geometry. As shown in Fig. 4(a), its Fourier spectrum exhibits a dispersionless flat band, a hallmark of the kagome geometry. The flatness further implies that at $\nu = 3/2$, corresponding to the zero–magnetic-field limit of the effective Ising model, the system hosts quasi-degenerate ground states that reflect strong charge fluctuations (Appendix VI 1 [162]). In this limit, the kagome Ising model with nearest-neighbor coupling is known to exhibit a classical spin-liquid phase [193, 194], where "spin" refers to the charge occupation degrees of freedom. Such a classical spin liquid phase is characterized by a non-zero entropy appearing at zero temperature, indicating strong fluctuations of the classical Ising variables.

To confirm this prediction under realistic conditions, we perform cluster mean-field simulations incorporating the full range of interactions for the smallest twist angle $\theta = 3.89°$ (Appendix VI 1 [162]). The resulting entropy landscape, illustrated in Fig. 4(b), reveals an enhancement of entropy near $\nu = 3/2$, which corresponds to the zero magnetic field limit of the kagome Ising model. This finite entropy persists over an extended temperature range, signaling the robust charge fluctuations characteristic of the liquid state. At integer fillings $\nu = 1, 2, 3$, the entropy is quenched at relatively higher temperatures due to the formation of a valley-polarized state. Since the Wannier centers of the three valleys are spatially offset from one another, electrons tend to occupy the same valley to minimize inter-valley density repulsion (Appendix VI 1b [162]). Nevertheless, the classical spin liquid regime remains a dominant feature at intermediate temperatures, demonstrating that the geometric frustration of the kagome lattice drives exotic charge correlations in AB-stacked twisted $SnSe_2$.

Summary and discussion. In this work, we have established twisted $SnSe_2$ as a tunable platform for realizing stacking-dependent correlated physics, where the choice of stacking configuration acts as a switch between distinct lattice geometries. In the AA-stacked configuration, the system effectively undergoes dimensional reduction: it is described by a three-orbital triangular lattice where a non-symmorphic symmetry enforces quasi-1D hopping. By solving the resulting strong-coupling spin model, we identified a rich landscape of quantum phases, including a dimerized phase with finite entropy, valence-bond solids, and a quantum paramagnetic state. In the AB-stacked configuration, the system forms a kagome lattice model, where three sublattices originate from three valleys. In the strong coupling regime, we demonstrate that the interplay between geometric frustration and strong interactions stabilizes a classical spin liquid phase.

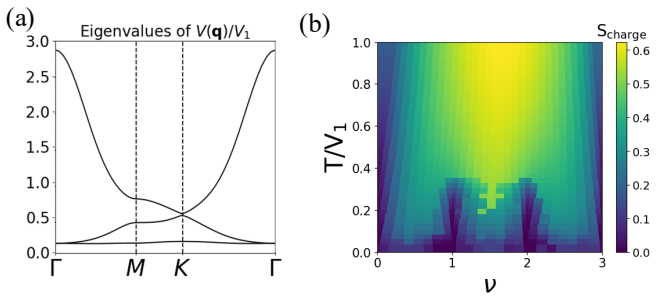

Figure 4. (a) Eigenvalues of the density-density interaction matrix, $V_{\eta\eta'}(\mathbf{q})$ (obtained from the realistic models), for AB-stacked $SnSe_2$ (see Appendix VI 1a [162]). (b) Entropy from charge fluctuations S_{charge} at various fillings ν (per moiré unit cell) and temperatures T for the smallest angle, $\theta = 3.89°$, for AB stacking. V_1 denotes the strength of nearest-neighbor density-density interactions (cf. Table S5 [162]).

We emphasize that the exotic phase identified in the idealized limits are not artifacts of simplification but remain robust against the complexity of realistic materials. For the AA-stacked case, our unrestricted Hartree–Fock calculations, which retain the full long-range couplings, confirm that the antiferromagnetic correlations driven by Heisenberg exchange remain the dominant ground-state property over an extensive parameter regime. In addition, the robustness of the exotic phase against weak perturbations has been analyzed and confirmed, as demonstrated in Appendix V 2f and V 3e [162]. Similarly, for the AB-stacked case, our cluster mean-field analysis explicitly incorporates realistic long-range interactions beyond the nearest-neighbor kagome model and confirms that the predicted phases are robust against realistic material imperfections. Encouragingly, preliminary experimental observations [195] have detected insulating behavior at integer fillings, providing initial support for the correlated insulating phases predicted by our theory.

Finally, twisted $SnSe_2$ structures are experimentally accessible [145], with the twist angles studied here well within achievable ranges. The remarkable tunability of the moiré system, where the electronic filling is controlled by gating and the ratio of interaction to kinetic energy is tuned by the twist angle and gate distance, enables a systematic exploration of correlated phase diagrams. While the effective dielectric constant in such 2D heterostructures is sensitive to the environment, we expect our identified phases to be robust against perturbations,

persisting over a finite range of interaction strengths. Consequently, we anticipate that the parameter regimes hosting these novel correlated phases are experimentally reachable. Our study thus provides the first theoretical framework for twisted $SnSe_2$, predicting a range of exotic quantum phases poised for experimental realization.

ACKNOWLEDGMENTS

B.A.B. and H.H. were supported by the Gordon and Betty Moore Foundation through Grant No. GBMF8685 towards the Princeton theory program, the Gordon and Betty Moore Foundation's EPiQS Initiative (Grant No. GBMF11070), the Office of Naval Research (ONR Grant No. N00014-20-1-2303), the Global Collaborative Network Grant at Princeton University, the Simons Investigator Grant No. 404513, the NSF-MERSEC (Grant No. MERSEC DMR 2011750), the Simons Collaboration on New Frontiers in Superconductivity (Grant No. SFI-MPS-NFS-00006741-01), the Princeton collaborative network, and the Schmidt Foundation at the Princeton University. M.L. and H.Y. were supported in part by the NSFC under Grant Nos. 12347107 and 12334003, and by MOSTC under Grant No. 2021YFA1400100. H.Y. acknowledges the support in part by the New Cornerstone Science Foundation through the Xplorer Prize. Y.J. was supported by the European Research Council (ERC) under the European Union's Horizon 2020 research and innovation program (Grant Agreement No. 101020833), as well as by the IKUR Strategy under the collaboration agreement between Ikerbasque Foundation and DIPC on behalf of the Department of Education of the Basque Government. H.P. was supported by the Ministry for Digital Transformation and of Civil Service of the Spanish Government through the QUANTUM ENIA project call - Quantum Spain project, and by the European Union through the Recovery, Transformation and Resilience Plan - NextGenerationEU within the framework of the Digital Spain 2026 Agenda. AF and DMK acknowledge funding by the DFG within the Priority Program SPP 2244 "2DMP" – 443274199. D.C. and S.A.P. acknowledge support from the UKRI Horizon Europe Guarantee Grant No. EP/Z002419/1 (for an ERC Consolidator Grant to S.A.P.). D.C. also gratefully acknowledges the support provided by the Leverhulme Trust. M.G.V received financial support from the Canada Excellence Research Chairs Program for Topological Quantum Matter, ID2022-142008NB-I00 projects funded by MICIU/AEI/10.13039/501100011033 and FEDER, UE and Diputacion Foral de Gipuzkoa Programa Mujeres y Ciencia.

[1] E. Y. Andrei, D. K. Efetov, P. Jarillo-Herrero, A. H. MacDonald, K. F. Mak, T. Senthil, E. Tutuc, A. Yazdani, and A. F. Young, Nat Rev Mater **6**, 201 (2021).
[2] D. M. Kennes, M. Claassen, L. Xian, A. Georges, A. J. Millis, J. Hone, C. R. Dean, D. N. Basov, A. N. Pasupathy, and A. Rubio, Nat. Phys. **17**, 155 (2021).
[3] A. Castellanos-Gomez, X. Duan, Z. Fei, H. R. Gutierrez, Y. Huang, X. Huang, J. Quereda, Q. Qian, E. Sutter, and P. Sutter, Nature Reviews Methods Primers **2**, 58 (2022).
[4] K. F. Mak and J. Shan, Nature Nanotechnology **17**, 686 (2022).
[5] Y. Jiang, U. Petralanda, G. Skorupskii, Q. Xu, H. Pi, D. Călugăru, H. Hu, J. Xie, R. A. Mustaf, P. Höhn, V. Haase, M. G. Vergniory, M. Claassen, L. Elcoro, N. Regnault, J. Shan, K. F. Mak, D. K. Efetov, E. Morosan, D. M. Kennes, A. Rubio, L. Xian, C. Felser, L. M. Schoop, and B. A. Bernevig, 2d theoretically twistable material database (2024), arXiv:2411.09741 [cond-mat.mtrl-sci].
[6] R. Bistritzer and A. H. MacDonald, PNAS **108**, 12233 (2011).
[7] Y. Cao, V. Fatemi, S. Fang, K. Watanabe, T. Taniguchi, E. Kaxiras, and P. Jarillo-Herrero, Nature **556**, 43 (2018).
[8] M. Yankowitz, S. Chen, H. Polshyn, Y. Zhang, K. Watanabe, T. Taniguchi, D. Graf, A. F. Young, and C. R. Dean, Science **363**, 1059 (2019).
[9] X. Lu, P. Stepanov, W. Yang, M. Xie, M. A. Aamir, I. Das, C. Urgell, K. Watanabe, T. Taniguchi, G. Zhang, A. Bachtold, A. H. MacDonald, and D. K. Efetov, Nature **574**, 653 (2019).
[10] P. Stepanov, I. Das, X. Lu, A. Fahimniya, K. Watanabe, T. Taniguchi, F. H. L. Koppens, J. Lischner, L. Levitov, and D. K. Efetov, Nature **583**, 375 (2020).
[11] Y. Saito, J. Ge, K. Watanabe, T. Taniguchi, and A. F. Young, Nat. Phys. **16**, 926 (2020).
[12] F. K. de Vries, E. Portolés, G. Zheng, T. Taniguchi, K. Watanabe, T. Ihn, K. Ensslin, and P. Rickhaus, Nat. Nanotechnol. **16**, 760 (2021).
[13] M. Oh, K. P. Nuckolls, D. Wong, R. L. Lee, X. Liu, K. Watanabe, T. Taniguchi, and A. Yazdani, Nature **600**, 240 (2021).
[14] H. Tian, X. Gao, Y. Zhang, S. Che, T. Xu, P. Cheung, K. Watanabe, T. Taniguchi, M. Randeria, F. Zhang, C. N. Lau, and M. W. Bockrath, Nature **614**, 440 (2023).
[15] G. Di Battista, P. Seifert, K. Watanabe, T. Taniguchi, K. C. Fong, A. Principi, and D. K. Efetov, Nano Lett. **22**, 6465 (2022).
[16] D. Călugăru, N. Regnault, M. Oh, K. P. Nuckolls, D. Wong, R. L. Lee, A. Yazdani, O. Vafek, and B. A. Bernevig, Phys. Rev. Lett. **129**, 117602 (2022).
[17] G. Chen, A. L. Sharpe, E. J. Fox, Y.-H. Zhang, S. Wang, L. Jiang, B. Lyu, H. Li, K. Watanabe, T. Taniguchi, Z. Shi, T. Senthil, D. Goldhaber-Gordon, Y. Zhang, and F. Wang, Nature **579**, 56 (2020).
[18] Y. Cao, V. Fatemi, A. Demir, S. Fang, S. L. Tomarken, J. Y. Luo, J. D. Sanchez-Yamagishi, K. Watanabe, T. Taniguchi, E. Kaxiras, R. C. Ashoori, and P. Jarillo-

Herrero, Nature **556**, 80 (2018).
[19] A. Kerelsky, L. J. McGilly, D. M. Kennes, L. Xian, M. Yankowitz, S. Chen, K. Watanabe, T. Taniguchi, J. Hone, C. Dean, A. Rubio, and A. N. Pasupathy, Nature **572**, 95 (2019).
[20] Y. Xie, B. Lian, B. Jäck, X. Liu, C.-L. Chiu, K. Watanabe, T. Taniguchi, B. A. Bernevig, and A. Yazdani, Nature **572**, 101 (2019).
[21] A. L. Sharpe, E. J. Fox, A. W. Barnard, J. Finney, K. Watanabe, T. Taniguchi, M. A. Kastner, and D. Goldhaber-Gordon, Science **365**, 605 (2019).
[22] Y. Jiang, X. Lai, K. Watanabe, T. Taniguchi, K. Haule, J. Mao, and E. Y. Andrei, Nature **573**, 91 (2019).
[23] Y. Choi, J. Kemmer, Y. Peng, A. Thomson, H. Arora, R. Polski, Y. Zhang, H. Ren, J. Alicea, G. Refael, F. von Oppen, K. Watanabe, T. Taniguchi, and S. Nadj-Perge, Nat. Phys. **15**, 1174 (2019).
[24] H. Polshyn, M. Yankowitz, S. Chen, Y. Zhang, K. Watanabe, T. Taniguchi, C. R. Dean, and A. F. Young, Nat. Phys. **15**, 1011 (2019).
[25] M. Serlin, C. L. Tschirhart, H. Polshyn, Y. Zhang, J. Zhu, K. Watanabe, T. Taniguchi, L. Balents, and A. F. Young, Science **367**, 900 (2020).
[26] D. Wong, K. P. Nuckolls, M. Oh, B. Lian, Y. Xie, S. Jeon, K. Watanabe, T. Taniguchi, B. A. Bernevig, and A. Yazdani, Nature **582**, 198 (2020).
[27] Y. Choi, H. Kim, Y. Peng, A. Thomson, C. Lewandowski, R. Polski, Y. Zhang, H. S. Arora, K. Watanabe, T. Taniguchi, J. Alicea, and S. Nadj-Perge, arXiv:2008.11746 [cond-mat] (2020), arXiv:2008.11746 [cond-mat].
[28] K. P. Nuckolls, M. Oh, D. Wong, B. Lian, K. Watanabe, T. Taniguchi, B. A. Bernevig, and A. Yazdani, Nature **588**, 610 (2020).
[29] Y. Choi, H. Kim, Y. Peng, A. Thomson, C. Lewandowski, R. Polski, Y. Zhang, H. S. Arora, K. Watanabe, T. Taniguchi, J. Alicea, and S. Nadj-Perge, Nature **589**, 536 (2021).
[30] Y. Saito, J. Ge, L. Rademaker, K. Watanabe, T. Taniguchi, D. A. Abanin, and A. F. Young, Nat. Phys. **17**, 478 (2021).
[31] X. Liu, Z. Wang, K. Watanabe, T. Taniguchi, O. Vafek, and J. I. A. Li, Science **371**, 1261 (2021).
[32] J. M. Park, Y. Cao, K. Watanabe, T. Taniguchi, and P. Jarillo-Herrero, Nature **592**, 43 (2021).
[33] S. Wu, Z. Zhang, K. Watanabe, T. Taniguchi, and E. Y. Andrei, Nat. Mater. **20**, 488 (2021).
[34] Y. Cao, D. Rodan-Legrain, J. M. Park, N. F. Q. Yuan, K. Watanabe, T. Taniguchi, R. M. Fernandes, L. Fu, and P. Jarillo-Herrero, Science **372**, 264 (2021).
[35] I. Das, X. Lu, J. Herzog-Arbeitman, Z.-D. Song, K. Watanabe, T. Taniguchi, B. A. Bernevig, and D. K. Efetov, Nat. Phys. **17**, 710 (2021).
[36] C. L. Tschirhart, M. Serlin, H. Polshyn, A. Shragai, Z. Xia, J. Zhu, Y. Zhang, K. Watanabe, T. Taniguchi, M. E. Huber, and A. F. Young, Science **372**, 1323 (2021).
[37] A. T. Pierce, Y. Xie, J. M. Park, E. Khalaf, S. H. Lee, Y. Cao, D. E. Parker, P. R. Forrester, S. Chen, K. Watanabe, T. Taniguchi, A. Vishwanath, P. Jarillo-Herrero, and A. Yacoby, Nat. Phys. **17**, 1210 (2021).
[38] P. Stepanov, M. Xie, T. Taniguchi, K. Watanabe, X. Lu, A. H. MacDonald, B. A. Bernevig, and D. K. Efetov, Phys. Rev. Lett. **127**, 197701 (2021).
[39] Y. Choi, H. Kim, C. Lewandowski, Y. Peng, A. Thomson, R. Polski, Y. Zhang, K. Watanabe, T. Taniguchi, J. Alicea, and S. Nadj-Perge, Nat. Phys. **17**, 1375 (2021).
[40] Y. Xie, A. T. Pierce, J. M. Park, D. E. Parker, E. Khalaf, P. Ledwith, Y. Cao, S. H. Lee, S. Chen, P. R. Forrester, K. Watanabe, T. Taniguchi, A. Vishwanath, P. Jarillo-Herrero, and A. Yacoby, Nature **600**, 439 (2021).
[41] I. Das, C. Shen, A. Jaoui, J. Herzog-Arbeitman, A. Chew, C.-W. Cho, K. Watanabe, T. Taniguchi, B. A. Piot, B. A. Bernevig, and D. K. Efetov, Phys. Rev. Lett. **128**, 217701 (2022).
[42] K. P. Nuckolls, R. L. Lee, M. Oh, D. Wong, T. Soejima, J. P. Hong, D. Călugăru, J. Herzog-Arbeitman, B. A. Bernevig, K. Watanabe, T. Taniguchi, N. Regnault, M. P. Zaletel, and A. Yazdani, Nature **620**, 525 (2023).
[43] J. Yu, B. A. Foutty, Y. H. Kwan, M. E. Barber, K. Watanabe, T. Taniguchi, Z.-X. Shen, S. A. Parameswaran, and B. E. Feldman, Nat. Commun. **14**, 6679 (2023), arXiv:2206.11304 [cond-mat].
[44] S. L. Tomarken, Y. Cao, A. Demir, K. Watanabe, T. Taniguchi, P. Jarillo-Herrero, and R. C. Ashoori, Phys. Rev. Lett. **123**, 046601 (2019).
[45] Y. Cao, D. Chowdhury, D. Rodan-Legrain, O. Rubies-Bigorda, K. Watanabe, T. Taniguchi, T. Senthil, and P. Jarillo-Herrero, Phys. Rev. Lett. **124**, 076801 (2020).
[46] U. Zondiner, A. Rozen, D. Rodan-Legrain, Y. Cao, R. Queiroz, T. Taniguchi, K. Watanabe, Y. Oreg, F. von Oppen, A. Stern, E. Berg, P. Jarillo-Herrero, and S. Ilani, Nature **582**, 203 (2020).
[47] S. Lisi, X. Lu, T. Benschop, T. A. de Jong, P. Stepanov, J. R. Duran, F. Margot, I. Cucchi, E. Cappelli, A. Hunter, A. Tamai, V. Kandyba, A. Giampietri, A. Barinov, J. Jobst, V. Stalman, M. Leeuwenhoek, K. Watanabe, T. Taniguchi, L. Rademaker, S. J. van der Molen, M. P. Allan, D. K. Efetov, and F. Baumberger, Nat. Phys. **17**, 189 (2021).
[48] T. Benschop, T. A. de Jong, P. Stepanov, X. Lu, V. Stalman, S. J. van der Molen, D. K. Efetov, and M. P. Allan, Phys. Rev. Res. **3**, 013153 (2021).
[49] B. Lian, Nature **592**, 191 (2021).
[50] A. Rozen, J. M. Park, U. Zondiner, Y. Cao, D. Rodan-Legrain, T. Taniguchi, K. Watanabe, Y. Oreg, A. Stern, E. Berg, P. Jarillo-Herrero, and S. Ilani, Nature **592**, 214 (2021).
[51] Y. Saito, F. Yang, J. Ge, X. Liu, T. Taniguchi, K. Watanabe, J. I. A. Li, E. Berg, and A. F. Young, Nature **592**, 220 (2021).
[52] X. Lu, B. Lian, G. Chaudhary, B. A. Piot, G. Romagnoli, K. Watanabe, T. Taniguchi, M. Poggio, A. H. MacDonald, B. A. Bernevig, and D. K. Efetov, PNAS **118**, e2100006118 (2021).
[53] N. C. H. Hesp, I. Torre, D. Rodan-Legrain, P. Novelli, Y. Cao, S. Carr, S. Fang, P. Stepanov, D. Barcons-Ruiz, H. Herzig Sheinfux, K. Watanabe, T. Taniguchi, D. K. Efetov, E. Kaxiras, P. Jarillo-Herrero, M. Polini, and F. H. L. Koppens, Nat. Phys. **17**, 1162 (2021).
[54] J. Díez-Mérida, A. Díez-Carlón, S. Y. Yang, Y.-M. Xie, X.-J. Gao, J. Senior, K. Watanabe, T. Taniguchi, X. Lu, A. P. Higginbotham, K. T. Law, and D. K. Efetov, Nat. Commun. **14**, 2396 (2023).
[55] S. Hubmann, P. Soul, G. Di Battista, M. Hild,

K. Watanabe, T. Taniguchi, D. K. Efetov, and S. D. Ganichev, Phys. Rev. Mater. **6**, 024003 (2022).
[56] B. Ghawri, P. S. Mahapatra, M. Garg, S. Mandal, S. Bhowmik, A. Jayaraman, R. Soni, K. Watanabe, T. Taniguchi, H. R. Krishnamurthy, M. Jain, S. Banerjee, U. Chandni, and A. Ghosh, Nat. Commun. **13**, 1522 (2022).
[57] A. Jaoui, I. Das, G. Di Battista, J. Díez-Mérida, X. Lu, K. Watanabe, T. Taniguchi, H. Ishizuka, L. Levitov, and D. K. Efetov, Nat. Phys. **18**, 633 (2022).
[58] A. K. Paul, A. Ghosh, S. Chakraborty, U. Roy, R. Dutta, K. Watanabe, T. Taniguchi, A. Panda, A. Agarwala, S. Mukerjee, S. Banerjee, and A. Das, Nat. Phys. **18**, 691 (2022).
[59] S. Grover, M. Bocarsly, A. Uri, P. Stepanov, G. Di Battista, I. Roy, J. Xiao, A. Y. Meltzer, Y. Myasoedov, K. Pareek, K. Watanabe, T. Taniguchi, B. Yan, A. Stern, E. Berg, D. K. Efetov, and E. Zeldov, Nat. Phys. **18**, 885 (2022).
[60] X.-F. Zhou, Y.-W. Liu, C.-Y. Hao, C. Yan, Q. Zheng, Y.-N. Ren, Y.-X. Zhao, K. Watanabe, T. Taniguchi, and L. He, Phys. Rev. B **107**, 125410 (2023).
[61] Z.-D. Song and B. A. Bernevig, Phys. Rev. Lett. **129**, 047601 (2022).
[62] H. Hu, B. A. Bernevig, and A. M. Tsvelik, Phys. Rev. Lett. **131**, 026502 (2023).
[63] H. Hu, G. Rai, L. Crippa, J. Herzog-Arbeitman, D. Călugăru, T. Wehling, G. Sangiovanni, R. Valentí, A. M. Tsvelik, and B. A. Bernevig, Phys. Rev. Lett. **131**, 166501 (2023).
[64] G. Rai, L. Crippa, D. Călugăru, H. Hu, F. Paoletti, L. de' Medici, A. Georges, B. A. Bernevig, R. Valentí, G. Sangiovanni, and T. Wehling, Phys. Rev. X **14**, 031045 (2024).
[65] D. Călugăru, H. Hu, R. L. Merino, N. Regnault, D. K. Efetov, and B. A. Bernevig, arXiv:2402.14057 [cond-mat] (2024), arXiv:2402.14057 [cond-mat].
[66] J. Herzog-Arbeitman, D. Călugăru, J. Yu, H. Hu, N. Regnault, and B. A. Bernevig, To be published (2024).
[67] R. L. Merino, D. Calugaru, H. Hu, J. Diez-Merida, A. Diez-Carlon, T. Taniguchi, K. Watanabe, P. Seifert, B. A. Bernevig, and D. K. Efetov, arXiv:2402.11749 [cond-mat] 10.48550/arXiv.2402.11749 (2024), arXiv:2402.11749 [cond-mat].
[68] J. Yu, M. Xie, B. A. Bernevig, and S. Das Sarma, Phys. Rev. B **108**, 035129 (2023).
[69] S. Batlle-Porro, D. Calugaru, H. Hu, R. K. Kumar, N. C. H. Hesp, K. Watanabe, T. Taniguchi, B. A. Bernevig, P. Stepanov, and F. H. L. Koppens, arXiv:2402.00869 [cond-mat] 10.48550/arXiv.2402.12296 (2024), arXiv:2402.00869 [cond-mat].
[70] H. Shi and X. Dai, Phys. Rev. B **106**, 245129 (2022).
[71] Y.-Z. Chou and S. Das Sarma, Phys. Rev. Lett. **131**, 026501 (2023).
[72] C. Huang, X. Zhang, G. Pan, H. Li, K. Sun, X. Dai, and Z. Y. Meng, Phys. Rev. B **109**, 125404 (2024).
[73] J. Herzog-Arbeitman, J. Yu, D. Călugăru, H. Hu, N. Regnault, C. Liu, O. Vafek, P. Coleman, A. Tsvelik, Z. da Song, and B. A. Bernevig, Topological heavy fermion principle for flat (narrow) bands with concentrated quantum geometry (2024), arXiv:2404.07253 [cond-mat.str-el].
[74] K. Singh, A. Chew, J. Herzog-Arbeitman, B. A. Bernevig, and O. Vafek, Nature Communications **15**, 5257 (2024).
[75] T. Han, Z. Lu, G. Scuri, J. Sung, J. Wang, T. Han, K. Watanabe, T. Taniguchi, H. Park, and L. Ju, Nature Nanotechnology **19**, 181 (2024).
[76] Z. Lu, T. Han, Y. Yao, A. P. Reddy, J. Yang, J. Seo, K. Watanabe, T. Taniguchi, L. Fu, and L. Ju, Nature **626**, 759 (2024).
[77] Y. Choi, Y. Choi, M. Valentini, C. L. Patterson, L. F. W. Holleis, O. I. Sheekey, H. Stoyanov, X. Cheng, T. Taniguchi, K. Watanabe, and A. F. Young, Nature **639**, 342 (2025).
[78] T. Han, Z. Lu, Z. Hadjri, L. Shi, Z. Wu, W. Xu, Y. Yao, A. A. Cotten, O. S. Sedeh, H. Weldeyesus, J. Yang, J. Seo, S. Ye, M. Zhou, H. Liu, G. Shi, Z. Hua, K. Watanabe, T. Taniguchi, P. Xiong, D. M. Zumbühl, L. Fu, and L. Ju, Nature 10.1038/s41586-025-09169-7 (2025).
[79] A. Kerelsky, C. Rubio-Verdú, L. Xian, D. M. Kennes, D. Halbertal, N. Finney, L. Song, S. Turkel, L. Wang, K. Watanabe, T. Taniguchi, J. Hone, C. Dean, D. N. Basov, A. Rubio, and A. N. Pasupathy, Proceedings of the National Academy of Sciences **118**, e2017366118 (2021), https://www.pnas.org/doi/pdf/10.1073/pnas.2017366118.
[80] J. Herzog-Arbeitman, Y. Wang, J. Liu, P. M. Tam, Z. Qi, Y. Jia, D. K. Efetov, O. Vafek, N. Regnault, H. Weng, Q. Wu, B. A. Bernevig, and J. Yu, Phys. Rev. B **109**, 205122 (2024).
[81] Y. H. Kwan, J. Yu, J. Herzog-Arbeitman, D. K. Efetov, N. Regnault, and B. A. Bernevig, Moiré fractional chern insulators iii: Hartree-fock phase diagram, magic angle regime for chern insulator states, the role of the moiré potential and goldstone gaps in rhombohedral graphene superlattices (2023), arXiv:2312.11617 [cond-mat.str-el].
[82] J. Yu, J. Herzog-Arbeitman, Y. H. Kwan, N. Regnault, and B. A. Bernevig, Moiré fractional chern insulators iv: Fluctuation-driven collapse of fcis in multi-band exact diagonalization calculations on rhombohedral graphene (2024), arXiv:2407.13770 [cond-mat.str-el].
[83] K. Huang, X. Li, S. Das Sarma, and F. Zhang, Phys. Rev. B **110**, 115146 (2024).
[84] J. Dong, T. Wang, T. Wang, T. Soejima, M. P. Zaletel, A. Vishwanath, and D. E. Parker, Phys. Rev. Lett. **133**, 206503 (2024).
[85] Z. Dong, A. S. Patri, and T. Senthil, Phys. Rev. Lett. **133**, 206502 (2024).
[86] B. Zhou, H. Yang, and Y.-H. Zhang, Phys. Rev. Lett. **133**, 206504 (2024).
[87] E. Viñas Boström, A. Fischer, J. B. Profe, J. Zhang, D. M. Kennes, and A. Rubio, npj Computational Materials **10**, 163 (2024).
[88] Y. H. Kwan, T. Tan, and T. Devakul, Fractional chern mosaic in supermoiré graphene (2024), arXiv:2411.08880 [cond-mat.str-el].
[89] L.-Q. Xia, S. C. de la Barrera, A. Uri, A. Sharpe, Y. H. Kwan, Z. Zhu, K. Watanabe, T. Taniguchi, D. Goldhaber-Gordon, L. Fu, T. Devakul, and P. Jarillo-Herrero, Nature Physics **21**, 239 (2025).
[90] H. Park, J. Cai, E. Anderson, X.-W. Zhang, X. Liu, W. Holtzmann, W. Li, C. Wang, C. Hu, Y. Zhao, *et al.*, Nature Physics **21**, 549 (2025).

[91] B. A. Bernevig and Y. H. Kwan, "berry trashcan" model of interacting electrons in rhombohedral graphene (2025), arXiv:2503.09692 [cond-mat.str-el].

[92] H. Li, B. A. Bernevig, and N. Regnault, Multi-band exact diagonalization and an iteration approach to hunt for fractional chern insulators in rhombohedral multilayer graphene (2025), arXiv:2504.20140 [cond-mat.str-el].

[93] J. Xie, Z. Zhang, X. Chen, Y. H. Kwan, Z. Huo, J. Herzog-Arbeitman, L. Guo, K. Watanabe, T. Taniguchi, K. Liu, X. C. Xie, B. A. Bernevig, Z.-D. Song, and X. Lu, Unconventional orbital magnetism in graphene-based fractional chern insulators (2025), arXiv:2506.01485 [cond-mat.mes-hall].

[94] F. Wu, T. Lovorn, E. Tutuc, and A. H. MacDonald, Phys. Rev. Lett. **121**, 026402 (2018).

[95] Y. Tang, L. Li, T. Li, Y. Xu, S. Liu, K. Barmak, K. Watanabe, T. Taniguchi, A. H. MacDonald, J. Shan, and K. F. Mak, Nature **579**, 353 (2020).

[96] L. Wang, E.-M. Shih, A. Ghiotto, L. Xian, D. A. Rhodes, C. Tan, M. Claassen, D. M. Kennes, Y. Bai, B. Kim, K. Watanabe, T. Taniguchi, X. Zhu, J. Hone, A. Rubio, A. N. Pasupathy, and C. R. Dean, Nature Materials **19**, 861 (2020).

[97] L. Wei, Q. Li, M. U. Rehman, Y. He, D. An, S. Li, K. Watanabe, T. Taniguchi, M. Claassen, K. S. Novoselov, D. M. Kennes, A. Rubio, D. A. Rhodes, L. Xian, G. Yu, and L. Wang, Nature Communications **16**, 1185 (2025).

[98] Y.-M. Wu, Z. Wu, and H. Yao, Phys. Rev. Lett. **130**, 126001 (2023).

[99] Y. Guo, J. Pack, J. Swann, L. Holtzman, M. Cothrine, K. Watanabe, T. Taniguchi, D. Mandrus, K. Barmak, J. Hone, A. J. Millis, A. N. Pasupathy, and C. R. Dean, Superconductivity in twisted bilayer wse2 (2024), arXiv:2406.03418.

[100] Y. Xia, Z. Han, K. Watanabe, T. Taniguchi, J. Shan, and K. F. Mak, Nature , 1 (2024).

[101] L. Klebl, A. Fischer, L. Classen, M. M. Scherer, and D. M. Kennes, Phys. Rev. Res. **5**, L012034 (2023).

[102] J. Zhu, Y.-Z. Chou, M. Xie, and S. Das Sarma, Phys. Rev. B **111**, L060501 (2025).

[103] S. Kim, J. F. Mendez-Valderrama, X. Wang, and D. Chowdhury, Nature Communications **16**, 1701 (2025).

[104] D. Guerci, D. Kaplan, J. Ingham, J. H. Pixley, and A. J. Millis, Topological superconductivity from repulsive interactions in twisted wse_2 (2024), arXiv:2408.16075 [cond-mat.supr-con].

[105] W. Qin, W.-X. Qiu, and F. Wu, Kohn-luttinger mechanism of superconductivity in twisted bilayer wse_2: Gate-tunable unconventional pairing symmetry (2024), arXiv:2409.16114 [cond-mat.supr-con].

[106] C. Tuo, M.-R. Li, Z. Wu, W. Sun, and H. Yao, Theory of topological superconductivity and antiferromagnetic correlated insulators in twisted bilayer wse_2 (2024), arXiv:2409.06779 [cond-mat.str-el].

[107] A. V. Chubukov and C. M. Varma, Phys. Rev. B **111**, 014507 (2025).

[108] A. Fischer, L. Klebl, V. Crépel, S. Ryee, A. Rubio, L. Xian, T. O. Wehling, A. Georges, D. M. Kennes, and A. J. Millis, Theory of intervalley-coherent afm order and topological superconductivity in twisted wse_2 (2024), arXiv:2412.14296 [cond-mat.str-el].

[109] F. Xu, Z. Sun, J. Li, C. Zheng, C. Xu, J. Gao, T. Jia, K. Watanabe, T. Taniguchi, B. Tong, L. Lu, J. Jia, Z. Shi, S. Jiang, Y. Zhang, Y. Zhang, S. Lei, X. Liu, and T. Li, Signatures of unconventional superconductivity near reentrant and fractional quantum anomalous hall insulators (2025), arXiv:2504.06972 [cond-mat.mes-hall].

[110] C. Xu, N. Zou, N. Peshcherenko, A. Jahin, T. Li, S.-Z. Lin, and Y. Zhang, Chiral superconductivity from spin polarized chern band in twisted $mote_2$ (2025), arXiv:2504.07082 [cond-mat.supr-con].

[111] T. Li, S. Jiang, B. Shen, Y. Zhang, L. Li, Z. Tao, T. Devakul, K. Watanabe, T. Taniguchi, L. Fu, J. Shan, and K. F. Mak, Nature **600**, 641 (2021).

[112] T. Devakul and L. Fu, Phys. Rev. X **12**, 021031 (2022).

[113] Y.-M. Xie, C.-P. Zhang, J.-X. Hu, K. F. Mak, and K. T. Law, Phys. Rev. Lett. **128**, 026402 (2022).

[114] Z. Tao, B. Shen, S. Jiang, T. Li, L. Li, L. Ma, W. Zhao, J. Hu, K. Pistunova, K. Watanabe, T. Taniguchi, T. F. Heinz, K. F. Mak, and J. Shan, Phys. Rev. X **14**, 011004 (2024).

[115] N. Regnault and B. A. Bernevig, Phys. Rev. X **1**, 021014 (2011).

[116] Y.-L. Wu, B. A. Bernevig, and N. Regnault, Phys. Rev. B **85**, 075116 (2012).

[117] T. Li, S. Jiang, B. Shen, Y. Zhang, L. Li, Z. Tao, T. Devakul, K. Watanabe, T. Taniguchi, L. Fu, J. Shan, and K. F. Mak, Nature **600**, 641 (2021).

[118] F. Xu, Z. Sun, T. Jia, C. Liu, C. Xu, C. Li, Y. Gu, K. Watanabe, T. Taniguchi, B. Tong, J. Jia, Z. Shi, S. Jiang, Y. Zhang, X. Liu, and T. Li, Phys. Rev. X **13**, 031037 (2023).

[119] H. Park, J. Cai, E. Anderson, Y. Zhang, J. Zhu, X. Liu, C. Wang, W. Holtzmann, C. Hu, Z. Liu, T. Taniguchi, K. Watanabe, J.-H. Chu, T. Cao, L. Fu, W. Yao, C.-Z. Chang, D. Cobden, D. Xiao, and X. Xu, Nature **622**, 74 (2023).

[120] J. Cai, E. Anderson, C. Wang, X. Zhang, X. Liu, W. Holtzmann, Y. Zhang, F. Fan, T. Taniguchi, K. Watanabe, Y. Ran, T. Cao, L. Fu, D. Xiao, W. Yao, and X. Xu, Nature **622**, 63 (2023).

[121] Y. Zeng, Z. Xia, K. Kang, J. Zhu, P. Knüppel, C. Vaswani, K. Watanabe, T. Taniguchi, K. F. Mak, and J. Shan, Nature **622**, 69 (2023).

[122] V. Crépel and L. Fu, Phys. Rev. B **107**, L201109 (2023).

[123] A. P. Reddy, F. Alsallom, Y. Zhang, T. Devakul, and L. Fu, Phys. Rev. B **108**, 085117 (2023).

[124] A. P. Reddy and L. Fu, Phys. Rev. B **108**, 245159 (2023).

[125] C. Wang, X.-W. Zhang, X. Liu, Y. He, X. Xu, Y. Ran, T. Cao, and D. Xiao, Phys. Rev. Lett. **132**, 036501 (2024).

[126] Y. Jia, J. Yu, J. Liu, J. Herzog-Arbeitman, Z. Qi, H. Pi, N. Regnault, H. Weng, B. A. Bernevig, and Q. Wu, Phys. Rev. B **109**, 205121 (2024).

[127] J. Yu, J. Herzog-Arbeitman, M. Wang, O. Vafek, B. A. Bernevig, and N. Regnault, Phys. Rev. B **109**, 045147 (2024).

[128] L. Ju, A. H. MacDonald, K. F. Mak, J. Shan, and X. Xu, Nature Reviews Materials **9**, 455 (2024).

[129] C. Xu, J. Li, Y. Xu, Z. Bi, and Y. Zhang, Proceedings of the National Academy of Sciences of the United States of America **121**, 10.1073/pnas.2316749121 (2024).

[130] N. Morales-Durán, N. Wei, J. Shi, and A. H. MacDon-

ald, Phys. Rev. Lett. **132**, 096602 (2024).
[131] Y. Zhang, H. Pi, J. Liu, W. Miao, Z. Qi, N. Regnault, H. Weng, X. Dai, B. A. Bernevig, Q. Wu, and J. Yu, Universal moiré-model-building method without fitting: Application to twisted $mote_2$ and wse_2 (2024), arXiv:2411.08108 [cond-mat.mes-hall].
[132] M. Wang, X. Wang, and O. Vafek, Phys. Rev. B **110**, L201107 (2024).
[133] C. Wang, X.-W. Zhang, X. Liu, J. Wang, T. Cao, and D. Xiao, Phys. Rev. Lett. **134**, 076503 (2025).
[134] H. Park, W. Li, C. Hu, C. Beach, M. Gonçalves, J. F. Mendez-Valderrama, J. Herzog-Arbeitman, T. Taniguchi, K. Watanabe, D. Cobden, L. Fu, B. A. Bernevig, N. Regnault, J.-H. Chu, D. Xiao, and X. Xu, Observation of high-temperature dissipationless fractional chern insulator (2025), arXiv:2503.10989 [cond-mat.mes-hall].
[135] X. Chang, F. Liu, F. Xu, C. Xu, J. Xiao, Z. Sun, P. Jiao, Y. Zhang, S. Wang, B. Shen, R. He, K. Watanabe, T. Taniguchi, R. Zhong, J. Jia, Z. Shi, X. Liu, Y. Zhang, D. Qian, T. Li, and S. Jiang, Evidence of competing ground states between fractional chern insulator and antiferromagnetism in moiré mote2 (2025), arXiv:2503.13213 [cond-mat.mes-hall].
[136] M. Fujimoto and T. Kariyado, Phys. Rev. B **104**, 125427 (2021).
[137] P. Wang, G. Yu, Y. H. Kwan, Y. Jia, S. Lei, S. Klemenz, F. A. Cevallos, R. Singha, T. Devakul, K. Watanabe, T. Taniguchi, S. L. Sondhi, R. J. Cava, L. M. Schoop, S. A. Parameswaran, and S. Wu, Nature **605**, 57 (2022).
[138] L. Wei, Q. Xu, Y. He, Q. Li, Y. Huang, W. Zhu, K. Watanabe, T. Taniguchi, M. Claassen, D. A. Rhodes, D. M. Kennes, L. Xian, A. Rubio, and L. Wang, Proceedings of the National Academy of Sciences **121**, e2321665121 (2024), https://www.pnas.org/doi/pdf/10.1073/pnas.2321665121.
[139] Q. J. Zong, H. Wang, Q. Zhang, X. Cheng, Y. He, Q. Xu, A. Fischer, K. Watanabe, T. Taniguchi, D. A. Rhodes, L. Xian, D. M. Kennes, A. Rubio, G. Yu, and L. Wang, Nature Communications **16**, 4058 (2025).
[140] F. Wu, T. Lovorn, E. Tutuc, I. Martin, and A. H. MacDonald, Phys. Rev. Lett. **122**, 086402 (2019).
[141] T. Devakul, V. Crépel, Y. Zhang, and L. Fu, Nat. Commun. **12**, 6730 (2021).
[142] X.-W. Zhang, C. Wang, X. Liu, Y. Fan, T. Cao, and D. Xiao, Nat Commun **15**, 4223 (2024).
[143] M. Angeli and A. H. MacDonald, PNAS **118**, e2021826118 (2021).
[144] M. Claassen, L. Xian, D. M. Kennes, and A. Rubio, Nat. Commun. **13**, 4915 (2022).
[145] D. Călugăru, Y. Jiang, H. Hu, H. Pi, J. Yu, M. G. Vergniory, J. Shan, C. Felser, L. M. Schoop, D. K. Efetov, K. F. Mak, and B. A. Bernevig, Nature **643**, 376 (2025).
[146] T. Kariyado, Phys. Rev. B **107**, 085127 (2023).
[147] P. M. Eugenio, Z.-X. Luo, A. Vishwanath, and P. A. Volkov, Tunable $t - t' - u$ hubbard models in twisted square homobilayers (2025), arXiv:2406.02448 [cond-mat.str-el].
[148] C. Lei, P. T. Mahon, and A. H. MacDonald, arXiv preprint arXiv:2411.18828 (2024).
[149] Y. Jiang, U. Petralanda, G. Skorupskii, Q. Xu, H. Pi, D. Călugăru, H. Hu, J. Xie, R. A. Mustaf, P. Höhn, V. Haase, M. G. Vergniory, M. Claassen, L. Elcoro, N. Regnault, J. Shan, K. F. Mak, D. K. Efetov, E. Morosan, D. M. Kennes, A. Rubio, L. Xian, C. Felser, L. M. Schoop, and B. A. Bernevig, arXiv:2411.09741 [cond-mat] 10.48550/arXiv.2411.09741 (2024), arXiv:2411.09741 [cond-mat].
[150] K. Bao, H. Wang, Z. Liu, and jing Wang, Anisotropic band flattening in twisted bilayer of m-valley mxenes (2024), arXiv:2412.19613 [cond-mat.mes-hall].
[151] Z.-X. Luo, A. Vishwanath, and T. Kariyado, Single-band square lattice hubbard model from twisted bilayer c568 (2025), arXiv:2502.19483 [cond-mat.str-el].
[152] W. Sun, C. Tuo, and H. Yao, Single-band triangular lattice hubbard model with tunable anisotropy from twisted diamond homobilayers (2025), arXiv:2503.19829 [cond-mat.str-el].
[153] M. Fujimoto, T. Kawakami, and M. Koshino, Phys. Rev. Res. **4**, 043209 (2022).
[154] C. Lei, P. T. Mahon, and A. H. MacDonald, Moiré band theory for m-valley twisted transition metal dichalcogenides (2024), arXiv:2411.18828 [cond-mat.mes-hall].
[155] Z. Wang, A. Alexandradinata, R. J. Cava, and B. A. Bernevig, Nature **532**, 189 (2016).
[156] G. de la Flor, B. Souvignier, G. Madariaga, and M. I. Aroyo, Acta Cryst. A **77**, 559 (2021).
[157] Z. Y. Chen, S. A. Yang, and Y. X. Zhao, Nat. Commun. **13**, 2215 (2022).
[158] C. Zhang, Z. Y. Chen, Z. Zhang, and Y. X. Zhao, Phys. Rev. Lett. **130**, 256601 (2023).
[159] Z. Xiao, J. Zhao, Y. Li, R. Shindou, and Z.-D. Song, Phys. Rev. X **14**, 031037 (2024).
[160] A. A. Soluyanov and D. Vanderbilt, Phys. Rev. B **85**, 115415 (2012).
[161] N. Marzari, A. A. Mostofi, J. R. Yates, I. Souza, and D. Vanderbilt, Rev. Mod. Phys. **84**, 1419 (2012).
[162] See Supplemental Material at https://journals.aps.org/authors/supplemental-material-instructions for additional derivations, numerical details, and supporting figures.
[163] B. Lian, Z.-D. Song, N. Regnault, D. K. Efetov, A. Yazdani, and B. A. Bernevig, Phys. Rev. B **103**, 205414 (2021).
[164] A. Laturia, M. L. Van de Put, and W. G. Vandenberghe, npj 2D Materials and Applications **2**, 6 (2018).
[165] T. Knobloch, Y. Y. Illarionov, F. Ducry, C. Schleich, S. Wachter, K. Watanabe, T. Taniguchi, T. Mueller, M. Waltl, M. Lanza, M. I. Vexler, M. Luisier, and T. Grasser, Nature Electronics **4**, 98 (2021).
[166] Y. Jiang, H. Hu, D. Călugăru, C. Felser, S. Blanco-Canosa, H. Weng, Y. Xu, and B. A. Bernevig, Phys. Rev. B **111**, 125163 (2025).
[167] G. Kresse and J. Furthmüller, Computational materials science **6**, 15 (1996).
[168] G. Kresse and J. Hafner, Physical Review B **48**, 13115 (1993).
[169] G. Kresse and J. Hafner, Physical review B **47**, 558 (1993).
[170] G. Kresse and J. Hafner, Physical Review B **49**, 14251 (1994).
[171] G. Kresse and J. Furthmüller, Physical review B **54**, 11169 (1996).
[172] S. Baroni and R. Resta, Physical Review B **33**, 7017 (1986).
[173] M. Gajdoš, K. Hummer, G. Kresse, J. Furthmüller, and

F. Bechstedt, Physical Review B—Condensed Matter and Materials Physics **73**, 045112 (2006).
[174] D. Călugăru *et al.* (2025), in preparation.
[175] V. J. Emery, E. Fradkin, S. A. Kivelson, and T. C. Lubensky, Phys. Rev. Lett. **85**, 2160 (2000).
[176] A. Vishwanath and D. Carpentier, Phys. Rev. Lett. **86**, 676 (2001).
[177] R. Mukhopadhyay, C. L. Kane, and T. C. Lubensky, Phys. Rev. B **63**, 081103 (2001).
[178] R. Mukhopadhyay, C. L. Kane, and T. C. Lubensky, Phys. Rev. B **64**, 045120 (2001).
[179] S. Sur and K. Yang, Phys. Rev. B **96**, 075131 (2017).
[180] J. Kang and O. Vafek, Phys. Rev. Lett. **122**, 246401 (2019).
[181] R. Orbach, Phys. Rev. **112**, 309 (1958).
[182] J. Des Cloizeaux and M. Gaudin, Journal of Mathematical Physics **7**, 1384 (1966).
[183] F. C. Alcaraz, M. N. Barber, M. T. Batchelor, R. Baxter, and G. Quispel, Journal of Physics A: mathematical and general **20**, 6397 (1987).
[184] M. T. Batchelor and C. Hamer, Journal of Physics A: Mathematical and General **23**, 761 (1990).
[185] U. Schollwöck, Annals of Physics **326**, 96 (2011), january 2011 Special Issue.
[186] R. Moessner and S. L. Sondhi, Phys. Rev. Lett. **86**, 1881 (2001).
[187] P. W. Kasteleyn, Physica **27**, 1209 (1961).
[188] P. W. Kasteleyn, Journal of Mathematical Physics **4**, 287 (1963).
[189] P. Fendley, R. Moessner, and S. L. Sondhi, Phys. Rev. B **66**, 214513 (2002).
[190] A. Szasz and J. Motruk, Phys. Rev. B **103**, 235132 (2021).
[191] M. Bocquet, F. H. L. Essler, A. M. Tsvelik, and A. O. Gogolin, Phys. Rev. B **64**, 094425 (2001).
[192] T. Giamarchi and A. M. Tsvelik, Phys. Rev. B **59**, 11398 (1999).
[193] K. Kanô and S. Naya, Progress of theoretical physics **10**, 158 (1953).
[194] G. H. Wannier, Phys. Rev. **79**, 357 (1950).
[195] Z. Xia *et al.* (2025), in preparation.